Inorganic Chemistry

Article

pubs.acs.org/IC

A Nitrate Nonlinear Optical Crystal $Pb_{16}(OH)_{16}(NO_3)_{16}$ with a Large Second-Harmonic Generation Response

Lixian Chang,[†] Li Wang,*[,†] Xin Su,[‡] Shilie Pan,*[,‡] Reshalaiti Hailili,[†] Hongwei Yu,[‡] and Zhihua Yang[‡]

[†]College of Chemistry and Chemical Engineering, Xinjiang Normal University, Urumqi 830054, China

[‡]Key Laboratory of Functional Materials and Devices for Special Environments of Chinese Academy of Sciences, Xinjiang Key Laboratory of Electronic Information Materials and Devices, Xinjiang Technical Institute of Physics and Chemistry of Chinese Academy of Sciences, 40-1 South Beijing Road, Urumqi 830011, China

Supporting Information

ABSTRACT: A noncentrosymmetric nitrate, $Pb_{16}(OH)_{16}(NO_3)_{16}$, has been obtained using a hydrothermal method. It is constructed of $[Pb_4(OH)_4]^{4+}$ cubanes and nitrate form the overall three-dimensional structure via weak Pb−O bonds. Powder second-harmonic generation (SHG) using the Kurtz−Perry technique shows that $Pb_{16}(OH)_{16}(NO_3)_{16}$ is type I phase-matchable, and the measured SHG coefficient was 3.5 times that of KH_2PO_4. The direction and magnitude of the dipole moments in PbO_n polyhedra and $[NO_3]^-$ triangles of $Pb_{16}(OH)_{16}(NO_3)_{16}$ have been quantified using the bond-valence approach, which shows that the large SHG response originates from the cooperation of PbO_n polyhedra and $[NO_3]^-$ triangles. The band structure and density of states as well as electron density difference are calculated on the basis of density functional theory.

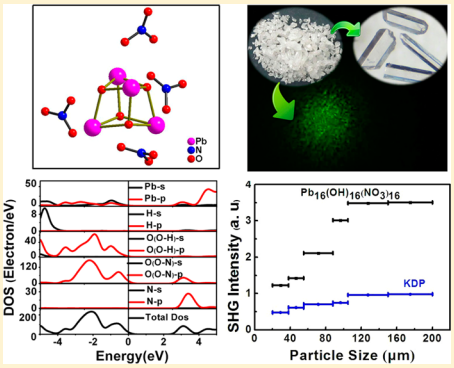

INTRODUCTION

Optical materials with second-order nonlinear optical (NLO) properties find uses in laser frequency conversion, as optical parameter oscillators, and as other optical and photonic devices.[1−7] A higher probability of acentricity of these materials is generally achieved by incorporating asymmetric building units into the molecular structures. In the well-known borate NLO systems, the macroscopic optical responses of the UV and deep-UV NLO borates are dominated by B−O units such as $[B_3O_6]^{3-}$ in β-BaB_2O_4 (BBO),[8] $[B_3O_7]^{5-}$ in LiB_3O_5 (LBO),[9] $[BO_3]^{3-}$ in $KBe_2BO_3F_2$ (KBBF)[10a] and $Sr_2Be_2B_2O_7$ (SBBO),[10b] and $[BO_4]^{5-}$ in SrB_4O_7.[7c] Among these B−O units, the planar $[BO_3]^{3-}$ anionic group possesses a relatively large microscopic second-order susceptibility; it is considered to be the best NLO effect for UV and deep-UV light generation. Analogous to the $[BO_3]^{3-}$ group, the $[CO_3]^{2-}$ and $[NO_3]^-$ structural units possess a number of unique advantages. (i) They always exist in the form of planar π-conjugated systems that can produce a moderate birefringence. (ii) A planar triangle structure together with their coparallel alignment may produce higher bulk NLO coefficients. Efforts to explore such advantages from materials with $[CO_3]^{2-}$ have been rewarding. For example, alkaline and alkaline earth fluoride carbonates $MNCO_3F$ (M = K, Rb, or Cs; N = Ca, Sr, or Ba)[11a] and $CsPbCO_3F$[11b] have been proven by Ye et al. to be promising UV NLO materials with potential in practical applications, despite their moderate second-harmonic generation (SHG) coefficients. However, in contrast to successful applications of borate, investigation of the NLO property of $[NO_3]^-$-containing materials has been scarcely investigated.[12]

In this work, we report the first example of lead nitrate hydroxide NLO crystal $Pb_{16}(OH)_{16}(NO_3)_{16}$ with a large SHG response. Interestingly, this compound displays a strong SHG response that is 3.5 times that of KH_2PO_4 (KDP), and it is type I phase-matchable. Furthermore, the direction and magnitude of the local dipole moments in PbO_n polyhedra and $[NO_3]^-$ triangles of $Pb_{16}(OH)_{16}(NO_3)_{16}$ have been quantified using a bond-valence method. Besides, to gain further insight into the electronic properties, the band structure, density of states, and electron density difference are calculated on the basis of the density functional theory (DFT). More importantly, such SHG behavior has not been reported previously for such a lead nitrate hydroxide compound.

EXPERIMENTAL SECTION

Synthesis. $Pb_{16}(OH)_{16}(NO_3)_{16}$ was prepared by hydrothermal synthesis. $Pb(NO_3)_2$ and $LiOH·H_2O$ used in this work were purchased from commercial sources without further treatment; 0.994 g (3.0 mmol) of $Pb(NO_3)_2$ and 0.020 g (0.5 mmol) of $LiOH·H_2O$ were suspended in 10.0 mL of deionized water and added to a stainless steel bomb equipped with a Teflon liner (23 mL). The mixture was heated at 200 °C for 72 h. After the mixture had cooled to 25 °C at a rate of 4 °C/h, the colorless block crystals of $Pb_{16}(OH)_{16}(NO_3)_{16}$ were collected and washed with deionized water. The yield was 92% based on lead.

Single-Crystal X-ray Diffraction. Single-crystal X-ray diffraction data were collected on an APEX II CCD diffractometer using monochromatic Mo Kα radiation (λ = 0.71073 Å) at 120(2) K,

Received: September 23, 2013
Published: March 11, 2014

   dx.doi.org/10.1021/ic402404a | Inorg. Chem. 2014, 53, 3320−3325

integrated with SAINT.[13] The structure was determined by the direct methods and refined by full-matrix least-squares fitting on F^2 using SHELXTL.[14] All non-hydrogen atoms were refined with anisotropic displacement parameters. The structure was checked with PLATON for missing symmetry elements.[15] Crystal data and details of data collection and refinement are summarized in Table 1. Atomic coordinates and selected bond distances and bond angles are listed in Tables S1–S3, respectively, of the Supporting Information. PXRD, IR, TG, and UV–vis–NIR diffuse reflectance spectra are shown in Figures S3–S6, respectively, of the Supporting Information.

Table 1. Crystal Data and Structural Refinement for $Pb_{16}(OH)_{16}(NO_3)_{16}$

empirical formula	$Pb_{16}(OH)_{16}(NO_3)_{16}$
formula weight	4579.33
temperature (K)	120(2)
wavelength (Å)	0.71073
crystal system	monoclinic
space group, Z	Cc, 4
unit cell dimensions	a = 25.4814(12) Å
	b = 17.1832(8) Å
	c = 18.1746(9) Å
	β = 133.54°
volume (Å^3)	5768.7(5)
density (calcd) (mg/m^3)	5.273
absorption coefficient (mm^{-1})	46.652
F(000)	7808
crystal size	0.06 mm × 0.02 mm × 0.02 mm
θ range for data collection (deg)	1.62–27.50
limiting indices	$-25 \le h \le 33$, $-22 \le k \le 22$, $-23 \le l \le 23$
no. of reflections collected/no. of unique reflections	21767/9192 [R(int) = 0.0766]
completeness to θ = 27.50° (%)	99.6
refinement method	full-matrix least-squares on F^2
goodness of fit on F^2	1.071
final R indices [$F_o^2 > 2\sigma(F_o^2)$][a]	R_1 = 0.0432, wR_2 = 0.0938
R indices (all data)[a]	R_1 = 0.0533, wR_2 = 0.1130
Flack parameter	0.49(2)
extinction coefficient	0.000053(4)
largest difference peak and hole	2.488 and −3.853 e/Å^3

[a] $R_1 = \sum||F_o| - |F_c||/\sum|F_o|$, and $wR_2 = [\sum w(F_o^2 - F_c^2)^2/\sum wF_o^4]^{1/2}$ for $F_o^2 > 2\sigma(F_o^2)$.

Powder X-ray Diffraction. The powder X-ray diffraction (PXRD) pattern of $Pb_{16}(OH)_{16}(NO_3)_{16}$ was obtained on a Bruker D8 ADVANCE X-ray diffractometer by using Cu Kα radiation (λ = 1.5418 Å) in the 2θ angular range of 10–80°.

Infrared Spectroscopy. An infrared spectrum was recorded on a Shimadzu IR Affinity-1 Fourier transform infrared spectrometer in the range from 400 to 4000 cm^{-1} with resolution of 2 cm^{-1}. The sample (6 mg) was mixed thoroughly with 500 mg of dried KBr.

TG Analysis. The TG curve was determined on a simultaneous NETZSCH STA 449F3 thermal analyzer instrument, with a heating rate of 10 °C/min in an atmosphere of flowing N_2 from 30 to 900 °C.

UV–Vis–NIR Diffuse Reflectance Spectrum. UV–vis–NIR diffuse reflection data were collected on a Shimadzu SolidSpec-3700DUV spectrophotometer over the range of 190–2600 nm.

Second-Order NLO Measurements. A second-harmonic generation test was performed on $Pb_{16}(OH)_{16}(NO_3)_{16}$ by the Kurtz–Perry method.[16] Polycrystalline $Pb_{16}(OH)_{16}(NO_3)_{16}$ was ground and sieved into distinct particle size ranges: <20, 20–38, 38–55, 55–88, 88–105, 105–150, and 150–200 μm. The polycrystalline powders were then placed in a light-tight box and irradiated with a Q-switched Nd:YAG solid-state laser of 1064 nm. To make relevant comparisons with known SHG materials, polycrystalline KDP was ground and sieved into the same particle size ranges.

Ferroelectric Measurements. To measure the potential ferroelectric behavior, frequency-dependent polarization measurements were taken at room temperature under a static electric field of 1–4 kV/cm between 50 and 200 Hz. The polarization measurements were taken on a Radiant Technologies model RT66A ferroelectric test system with a TREK high-voltage amplifier.

Calculation Details. The DFT calculation was performed using the CASTEP module.[17] The generalized gradient approximation (GGA) with the Ceperley and Alder-Perdew-Zunger functional (CA-PZ) functional was adopted.[18] The plane-wave basis set energy cutoff was set at 340.0 eV. The total energy tolerance was 2×10^{-6} eV/atom. The k-point grid sampling in the Monkhorst–Pack scheme was set at 2 × 2 × 2 for the Brillouin zone.

RESULTS AND DISCUSSION

Crystal Structure. Compound $Pb_{16}(OH)_{16}(NO_3)_{16}$ crystallizes in monoclinic noncentrosymmetric space group Cc, and the asymmetric units consist of 16 Pb atoms, 16 hydroxides, and 16 nitrates. Such a lead nitrate hydroxide has been previously reported,[19] and its structure was refined with space group Ia; however, the R values were high (R_1 = 0.076; wR_2 = 0.183). Hence, this paper provides improved refinements with an R_1 of <0.05. According to Davidovicha,[20] the limiting value for a Pb–O bond is considered to be 3.30 Å. The primary coordination sphere of the Pb(II) atom can be limited to the Pb–O distance of 2.70 Å, while the secondary coordination sphere ranges from 2.70 to 3.30 Å. Pb(1), Pb(3), and Pb(4) are ligated by three hydroxides in the primary coordination sphere and five oxygen atoms from nitrates in the secondary coordination sphere. The overall coordination number of these Pb atoms can be written as (3 + E) + 5, and the polyhedron in the primary coordination sphere is a ψ-tetrahedron. Pb(5) atoms have an overall coordination number of (3 + E) + 6, while Pb(8) atoms have an overall coordination number of (3 + E) + 4. The 10-coordinate Pb(2), Pb(6), and Pb(11) atoms have three hydroxides in the ψ-tetrahedral primary coordination sphere and seven oxygen atoms in the secondary coordination sphere. The eight-coordinate Pb(7), Pb(9), Pb(10), Pb(13), Pb(14), and Pb(16) atoms have four oxygen atoms from hydroxides and nitrate in the primary coordination sphere, with an overall coordination number of (4 + E) + 4. Pb(12) atoms have a coordination number of (4 + E) + 5, and their primary coordination spheres show a ψ-trigonal bipyramidal geometry. The Pb(15) atom has a unique coordination number of (4 + E) + 6. The view of the coordination environments of the 16 Pb atoms is shown in Figure 1. Table S4 of the Supporting Information gives the coordination number, coordination sphere geometry, and bond lengths of 16 Pb atoms in $Pb_{16}(OH)_{16}(NO_3)_{16}$. Only the primary coordination sphere is considered; the nitrate shows monodentate, bimonodentate, or free modes. When the secondary coordination sphere is also considered, the nitrate shows μ_3, μ_4, μ_5, and μ_6 modes, as shown in Figure S1 of the Supporting Information.

Simply, the overall three-dimensional structure of **1** can be viewed as being constructed of $[Pb_4(OH)_4]^{4+}$ cubanes and nitrate via weak Pb–O bonds (Figure S2 of the Supporting Information). Each $[Pb_4(OH)_4]^{4+}$ cubane consists of four Pb(II) atoms and four hydroxide ions that generate a distorted

dx.doi.org/10.1021/ic402404a | Inorg. Chem. 2014, 53, 3320–3325

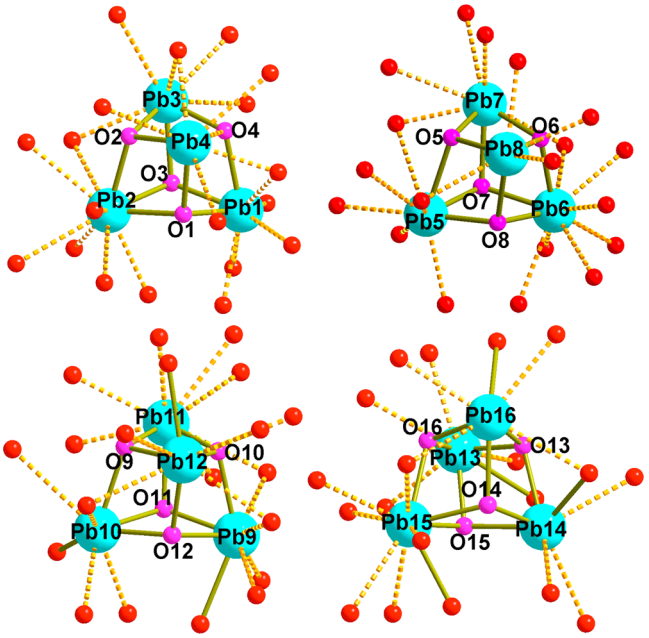

Figure 1. View of the coordination environments of Pb atoms. Note that the bonds linking Pb and oxygen atoms in the secondary sphere are shown as dashed orange lines.

cubane-shaped structure. Within a cubane, each Pb(II) atom is connected to three hydroxides and vice versa. The Pb−Pb distances range from 3.722(5) to 3.822(7) Å, and Pb−Pb−Pb angles are in the range of 57.888(2)−61.503(4)°. These values are in agreement with those of other $[Pb_4(OH)_4]^{4+}$ cubanelike structures reported previously. PXRD showed good agreement with the calculated one derived from the single-crystal data (Figure S3 of the Supporting Information).

Infrared Spectroscopy. The peaks around 3500 cm^{-1} can be attributed to the presence of hydroxyl groups. The peaks at 1385, 1307, 1029, and 820 cm^{-1} can be attributed to asymmetric stretching and symmetric stretching vibrations of $[NO_3]^-$ groups (Figure S4 of the Supporting Information).

TG Analysis. From the TG curve of Figure S5 of the Supporting Information, it can be seen that the material is very stable and there is no weight loss when the temperature is <150 °C. Then, it undergoes a weight loss between ~150 and 310 °C because of the release of the two molecules of H_2O. The observed weight loss of 3.17% matches well with the calculated one (3.14%). In the second stage, occurring between 310 and 900 °C, the weight loss might be attributed to the gradual decomposition of nitrate.

UV−Vis−NIR Diffuse Reflectance Spectroscopy. The UV cutoff edge of $Pb_{16}(OH)_{16}(NO_3)_{16}$ is below 310 nm (Figure S6 of the Supporting Information). The absorption (K/S) data are calculated from Kubelka−Munk function $F(R) = (1 - R)^2/2R = K/S$.[21] The absorption versus the energy of exciting light shows band gap energies of 3.78 eV.

Calculation. Figure 2 shows the obtained band structures for $Pb_{16}(OH)_{16}(NO_3)_{16}$ plotted along the high symmetry lines by the GGA calculations. $Pb_{16}(OH)_{16}(NO_3)_{16}$ is an indirect gap compound, with a calculated band gap of 2.779 eV, which is smaller than the experimental values mentioned above because of the well-known discontinuity in the derivative of exchange correlation energy within DFT.[22] The orbitals of $Pb_{16}(OH)_{16}(NO_3)_{16}$-calculated bands can be understood by analyzing the DOS diagrams. The upper region of the valence

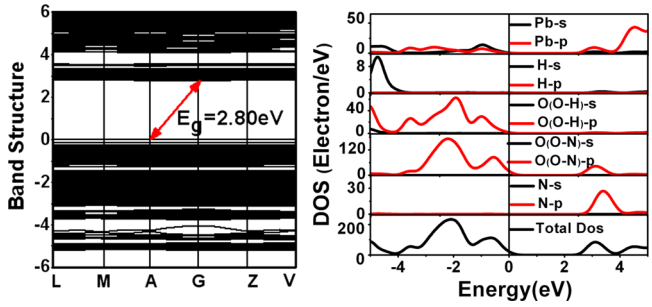

Figure 2. Calculated band structure and total density of states and the corresponding partial density of the orbital of $Pb_{16}(OH)_{16}(NO_3)_{16}$.

band is mainly composed of O 2p states, and the bottom of the conduction band is mainly composed of N 2p and O 2p states, which are hybridized. The O 2p states of the upper region of the valence band originate from both $[OH]^-$ and $[NO_3]^-$; the contributions of O 2p states from $[OH]^-$ and $[NO_3]^-$ are 27 and 73%, respectively.

In addition, to further verify the stereoactive lone pair electrons on the Pb^{2+} cation, the electron density difference map around the Pb^{2+} cation is calculated (Figure S7 of the Supporting Information). It shows that the $6s^2$ lone pair on the Pb^{2+} maintains its almost spherical shape, which indicates that the Pb^{2+} cation has an inert or non-stereoactive lone pair.

NLO and Ferroelectric Properties. Phase-matching experiments indicate that $Pb_{16}(OH)_{16}(NO_3)_{16}$ is type I phase-matchable,with large SHG responses, ~3.5 times that of the KDP standard with a similar grain size (Figure 3). A

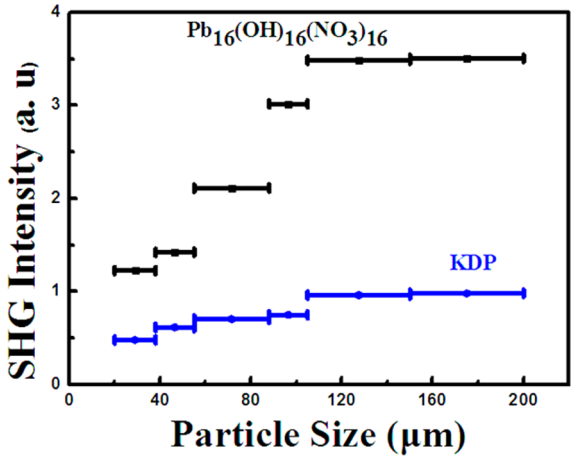

Figure 3. SHG measurements of $Pb_{16}(OH)_{16}(NO_3)_{16}$ ground crystals with KDP as a tester.

bond-valence method is used to calculate the direction and magnitude of the dipole moments in PbO_n polyhedra and $[NO_3]^-$ triangles of $Pb_{16}(OH)_{16}(NO_3)_{16}$.[23,24] The detailed calculation method and formula are described after Table S5 of the Supporting Information. Because the ELF calculations show that the $6s^2$ lone pair on the Pb^{2+} maintains its almost spherical shape, the distortion of the lone pair has not been considered. Here, both the primary coordination sphere of the Pb(II) atom with a Pb−O distance of 2.70 Å and the secondary coordination sphere that ranges from 2.70 to 3.30 Å are considered to ensure that the contribution of the Pb part to the dipole moment will not be underestimated. Furthermore, the cooperative action of the polyhedral dipoles has also been

dx.doi.org/10.1021/ic402404a | Inorg. Chem. 2014, 53, 3320−3325

Table 2. Detailed Contributions from PbO_n Polyhedra and $[NO_3]^-$ Triangles and Total Polarization of the Whole Unit Cell ($Z = 4$)

		dipole moment			
symmetric code	species	x	y	z	magnitude (D)
X, y, z	$\sum_{k=1}^{4}(PbO_n)_k$	5.0089	−1.2369	5.3963	4.3037
X, y, z	$\sum_{k=5}^{8}(PbO_n)_k$	8.0445	−5.2735	4.7288	7.9061
X, y, z	$\sum_{k=9}^{12}(PbO_n)_k$	0.0716	−2.9525	−2.0963	3.6501
X, y, z	$\sum_{k=13}^{16}(PbO_n)_k$	3.7768	1.2520	4.0747	3.3534
$0.5 + x, 1.5 - y, -0.5 + z$	$\sum_{k=1}^{4}(PbO_n)_k$	5.0089	1.2369	5.3963	4.3037
$0.5 + x, 1.5 - y, -0.5 + z$	$\sum_{k=5}^{8}(PbO_n)_k$	6.9139	4.4508	4.0593	6.2551
$0.5 + x, 1.5 - y, -0.5 + z$	$\sum_{k=9}^{12}(PbO_n)_k$	0.0716	2.9525	−2.0963	3.6501
$0.5 + x, 1.5 - y, -0.5 + z$	$\sum_{k=13}^{16}(PbO_n)_k$	3.7768	−1.2520	4.0747	3.3534
$X, 1 - y, -0.5 + z$	$\sum_{k=1}^{4}(PbO_n)_k$	4.4175	0.5640	4.6863	3.6455
$X, 1 - y, -0.5 + z$	$\sum_{k=5}^{8}(PbO_n)_k$	8.0445	5.2735	4.7288	7.9061
$X, 1 - y, -0.5 + z$	$\sum_{k=9}^{12}(PbO_n)_k$	0.0716	2.9525	−2.0963	3.6501
$X, 1 - y, -0.5 + z$	$\sum_{k=13}^{16}(PbO_n)_k$	3.7768	−1.2520	4.0747	3.3534
$0.5 + x, 0.5 + y, z$	$\sum_{k=1}^{4}(PbO_n)_k$	5.0089	−1.2369	5.3963	4.3037
$0.5 + x, 0.5 + y, z$	$\sum_{k=5}^{8}(PbO_n)_k$	8.0445	−5.2735	4.7288	7.9061
$0.5 + x, 0.5 + y, z$	$\sum_{k=9}^{12}(PbO_n)_k$	0.0716	−2.9525	−2.0963	3.6501
$0.5 + x, 0.5 + y, z$	$\sum_{k=13}^{16}(PbO_n)_k$	3.7768	1.2520	4.0747	3.3534
X, y, z	$\sum_{j=1}^{16}(NO_3)_j$	−7.4278	4.1265	−9.5338	8.0987
$0.5 + x, 1.5 - y, -0.5 + z$	$\sum_{j=1}^{16}(NO_3)_j$	−7.3913	−4.1396	−9.5236	8.0959
$X, 1 - y, -0.5 + z$	$\sum_{j=1}^{16}(NO_3)_j$	−7.3347	−4.1407	−9.5188	8.0882
$0.5 + x, 0.5 + y, z$	$\sum_{j=1}^{16}(NO_3)_j$	−7.3871	4.1444	−9.5262	8.0993
$Z = 4$	$\sum_{k=1}^{64}(PbO_n)_k$	65.8848	−1.4956	47.0343	47.8380

dx.doi.org/10.1021/ic402404a | Inorg. Chem. 2014, 53, 3320−3325

Table 2. continued

symmetric code	species	dipole moment			
		x	y	z	magnitude (D)
	$\sum_{j=1}^{64}(NO_3)_j$	−29.5408	−0.0094	−38.1023	27.8324
	total polarization	36.3440	-1.5050	8.9319	30.9186

evaluated using the complete crystal symmetry, including both point and translation operations. Not only the contribution from PbO_n polyhedra and $[NO_3]^-$ triangles of the asymmetric unit but also the total polarization of the whole unit cell ($Z = 4$) is included. The detailed calculation results are listed in Table 2 and Table S5 of the Supporting Information. From the table, we can see that the local dipole moment of PbO_n polyhedra in $Pb_{16}(OH)_{16}(NO_3)_{16}$ is 47.8380 D, which is larger than those of $[NO_3]^-$ triangles (27.8324 D). The SHG response of $Pb_{16}(OH)_{16}(NO_3)_{16}$ originates from the cooperation of PbO_n polyhedra and $[NO_3]^-$ triangles; the magnitudes of dipole moments along the b-axis are almost canceled, and their vector sum is well-enhanced in the $a-c$ plane. The total local dipole moment is 30.9186 D, with a net distortion for $Pb_{16}(OH)_{16}(NO_3)_{16}$ approximately along the [301] direction (Figure 4). The potential ferroelectric behavior and frequency-dependent polarization measurements were also conducted, and the observed curves do not show ferroelectric hysteresis, suggesting that the $Pb_{16}(OH)_{16}(NO_3)_{16}$ sample has no ferroelectric response (Figure S8 of the Supporting Information).

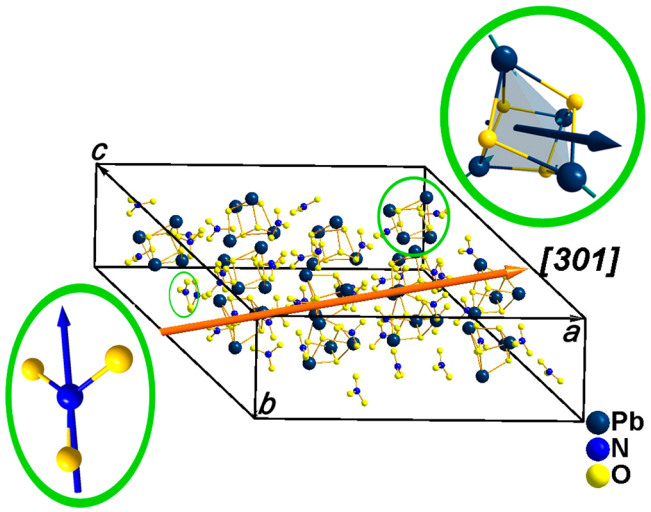

Figure 4. Orange arrow representing the direction of the net distortion along the [301] direction for $Pb_{16}(OH)_{16}(NO_3)_{16}$.

CONCLUSION

In summary, a nitrate nonlinear optical crystal $Pb_{16}(OH)_{16}(NO_3)_{16}$ is reported. Its crystal is constructed of $[Pb_4(OH)_4]^{4+}$ cubanes and the planar triangle π-conjugated $[NO_3]^-$ system. Powder SHG measurement shows that $Pb_{16}(OH)_{16}(NO_3)_{16}$ possesses a large SHG response ~3.5 times that of KDP and is type I phase-matchable. Further, the dipole moment and the first-principle calculations show that the SHG response of $Pb_{16}(OH)_{16}(NO_3)_{16}$ mainly originates from the cooperation of PbO_n polyhedra and $[NO_3]^-$ triangles. These indicate the nitrates with planar π-conjugated $[NO_3]^-$ triangles may be the potential candidates for the design of the UV NLO materials. In the future, we will find new NLO materials by combining building units containing second-order Jahn−Teller distorted cations with a planar π-conjugated system and understand the structural nature of their polarity.

ASSOCIATED CONTENT

Supporting Information

CIF file, final coordinates, selected bond distances, bond angles, XRD patterns, IR, UV−vis−NIR diffuse reflectance spectroscopy, TG, electron density difference map, calculation of distortion, and local dipole moment. This material is available free of charge via the Internet at http://pubs.acs.org.

AUTHOR INFORMATION

Corresponding Authors

*E-mail: slpan@ms.xjb.ac.cn. Phone: (86)991-3674558. Fax: (86)991-3838957.

*E-mail: wangliresearch@163.com.

Notes

The authors declare no competing financial interest.

ACKNOWLEDGMENTS

This work is supported by the 973 Program of China (Grant 2012CB626803), the National Natural Science Foundation of China (Grants U1129301, 51172277, 21101168, 21371147, 21365021, and 11104344), the Main Direction Program of Knowledge Innovation of the Chinese Academy of Sciences (Grant KJCX2-EW-H03-03), the One Hundred-Talent Progrm of the Chinese Academy of Sciences, the 12th Five-Year Plan Period (Grant 201130111), the High Technology Research & Development Program of Xinjiang (Grant 201116143), the Science and Technology Project of Urumqi (Grant G121130002), Xinjiang Science Funds for Distinguished Young Scientists (Grant 2013711009), and Inorganic chemistry key disciplines and Key Laboratory of Pollution Monitoring and Control of Xinjiang Normal University.

REFERENCES

(1) (a) Chen, C. T.; Wu, Y. C.; Jiang, A. D.; You, G. M.; Li, R.; Lin, S. L. *J. Opt. Soc. Am. B* **1989**, *6*, 616−621. (b) Becker, P. *Adv. Mater.* **1998**, *10*, 979−992. (c) Wei, Q. C.; Gunter, H.; Petri, K.; Margit, R.; Markus, H.; Hubert, H.; Gert, L. *J. Phys. Chem. B* **2012**, *116*, 1100−1110. (d) Hubert, H.; Stefanie, A. H.; Carmen, E. Z.; Stefan, L.; Oliver, O.; Ralf, R.; Isabel, K. *Chem. Mater.* **2009**, *21*, 2101−2107. (e) He, C.; Li, X. Z.; Wang, Z. J.; Long, X. F.; Mao, S. Y.; Ye, Z. G. *Chem. Mater.* **2010**, *22*, 5588−5592. (f) Wei, Q.; Wang, Z. J.; Li, X. Z.; Long, X. F.; Ye, Z. G. *Chem. Mater.* **2009**, *21*, 506−510.

(2) (a) Halasyamani, P. S.; Poeppelmeier, K. R. *Chem. Mater.* **1998**, *10*, 2753−2769. (b) Halasyamani, P. S. *Chem. Mater.* **2004**, *16*, 3586−3592. (c) Ra, H. S. K.; Ok, K. M.; Halasyamani, P. S. *J. Am. Chem. Soc.* **2003**, *125*, 7764−7765.

(3) (a) Maggard, P. A.; Stern, C. L.; Poeppelmeier, K. R. *J. Am. Chem. Soc.* **2001**, *123*, 7742−7743. (b) Donakowski, M. D.; Gautier, R.;

Yeon, J.; Moore, D. T.; Nino, J. C.; Halasyamani, P. S.; Poeppelmeier, K. R. *J. Am. Chem. Soc.* **2012**, *134*, 7679−7689. (c) Ok, K. M.; Chi, E. O.; Halasyamani, P. S. *Chem. Soc. Rev.* **2006**, *35*, 710−717.
(4) (a) Sun, C. F.; Hu, C. L.; Xu, X.; Yang, B. P.; Mao, J. G. *J. Am. Chem. Soc.* **2011**, *133*, 5561−5572. (b) Kong, F.; Huang, S. P.; Sun, Z. M.; Mao, J. G. *J. Am. Chem. Soc.* **2006**, *128*, 7750−7751.
(5) (a) Zhang, W. L.; Chen, W. D.; Zhang, H.; Geng, L.; Lin, C. S.; He, Z. Z. *J. Am. Chem. Soc.* **2010**, *132*, 1508−1509. (b) Wang, S. C.; Ye, N.; Li, W.; Zhao, D. *J. Am. Chem. Soc.* **2010**, *132*, 8779−8786. (c) Huang, Y. Z.; Wu, L. M.; Wu, X. T.; Li, L. H.; Chen, L.; Zhang, Y. F. *J. Am. Chem. Soc.* **2010**, *132*, 12788−12789.
(6) (a) Pan, S. L.; Smit, J. P.; Watkins, B.; Marvel, M. R.; Stern, C. L.; Poeppelmeier, K. R. *J. Am. Chem. Soc.* **2006**, *128*, 11631−11634. (b) Wu, H. P.; Yu, H. W.; Yang, Z. H.; Hou, X. L.; Su, X.; Pan, S. L.; Poeppelmeier, K. R.; Rondinelli, J. M. *J. Am. Chem. Soc.* **2013**, *135*, 4215−4218. (c) Wu, H. P.; Pan, S. L.; Poeppelmeier, K. R.; Li, H. Y.; Jia, D. Z.; Chen, Z. H.; Fan, X. Y.; Yang, Y.; Rondinelli, J. M.; Luo, H. S. *J. Am. Chem. Soc.* **2011**, *133*, 7786−7790. (d) Wu, H. P.; Yu, H. W.; Pan, S. L.; Huang, Z. J.; Yang, Z. H.; Su, X.; Poeppelmeier, K. R. *Angew. Chem., Int. Ed.* **2013**, *52*, 3406−3410.
(7) (a) Choyke, S. J.; Blau, S. M.; Larner, A. A.; Narducci, S. A.; Yeon, J.; Halasyamani, P. S.; Norquist, A. J. *Inorg. Chem.* **2009**, *48*, 11277−11282. (b) Hubbard, D. J.; Johnston, A. R.; Sanchez, C. H.; Narducci, S. A.; Norquis, A. J. *Inorg. Chem.* **2008**, *47*, 8518−8525. (c) Pan, F.; Shen, G. Q.; Wang, R. J.; Wang, X. Q.; Shen, D. Z. *J. Cryst. Growth* **2002**, *241*, 108−114.
(8) (a) Chen, C. T.; Wu, B. C.; Jiang, A. D.; You, G. M. *Sci. Sin., Ser. B (Engl. Ed.)* **1985**, *28*, 235−243. (b) Chen, C. T.; Xu, Z. Y.; Deng, D. Q.; Zhang, J.; Wong, G. K. *J. Appl. Phys. Lett.* **1996**, *68*, 2930−2932.
(9) Chen, C. T.; Ye, N.; Lin, J.; Jiang, J.; Zeng, W. R.; Wu, B. C. *Adv. Mater.* **1999**, *11*, 1071−1078.
(10) (a) Mei, L. F.; Wang, Y. B.; Chen, C. T.; Wu, B. C. *J. Appl. Phys.* **1993**, *74*, 7014−7015. (b) Chen, C. T.; Wang, Y. B.; Wu, B. C.; Wu, K. C.; Zeng, W. L.; Yu, L. H. *Nature* **1995**, *373*, 322−324.
(11) (a) Zou, G. H.; Ye, N.; Huang, L.; Lin, X. S. *J. Am. Chem. Soc.* **2011**, *133*, 20001−20007. (b) Zou, G. H.; Huang, L.; Ye, N.; Lin, C. S.; Cheng, W. D.; Huang, H. *J. Am. Chem. Soc.* **2013**, *135*, 18560−18566.
(12) (a) Dong, W. T.; Zhang, H. J.; Su, Q.; Lin, Y. H.; Wang, S. M.; Zhu, C. S. *J. Solid State Chem.* **1999**, *148*, 302−307. (b) Cong, R. H.; Yang, T.; Liao, F. H.; Wang, Y. X.; Lin, Z. H.; Lin, J. H. *Mater. Res. Bull.* **2012**, *47*, 2573−2578. (c) Sethuraman, K.; Babu, R. R.; Gopalakrishnan, R.; Ramasamy, P. *Cryst. Growth Des.* **2008**, *8*, 1863−1869.
(13) *SAINT*, version 7.60A; Bruker Analytical X-ray Instruments, Inc.: Madison, WI, 2008.
(14) Sheldrick, G. M. *SHELXTL*, version 6.14; Bruker Analytical X-ray Instruments, Inc.: Madison, WI, 2003.
(15) Spek, A. L. *J. Appl. Crystallogr.* **2003**, *36*, 7−13.
(16) (a) Kurtz, S.; Perry, K. T. T. *J. Appl. Phys.* **1968**, *39*, 3798−3813. (b) Dougherty, J. P.; Kurtz, S. K. *J. Appl. Crystallogr.* **1976**, *9*, 145−158.
(17) Clark, S. J.; Segall, M. D.; Pickard, C. J.; Hasnip, P. J.; Probert, M. J.; Rrfson, K.; Payne, M. C. *Z. Kristallogr.* **2005**, *220*, 567−570.
(18) (a) Ceperley, D. M.; Alder, B. J. *Phys. Rev. Lett.* **1980**, *45*, 566−569. (b) Perdew, J. P.; Zunger, A. *Phys. Rev. B* **1981**, *23*, 5048−5079.
(19) Grimes, S. M.; Johnston, S. R.; Abrahams, I. *J. Chem. Soc., Dalton Trans.* **1995**, *12*, 2081−2086.
(20) Davidovicha, R. L.; Stavilab, V.; Whitmirec, K. H. *Coord. Chem. Rev.* **2010**, *254*, 2193−2226.
(21) (a) Kubelka, P.; Munk, F. Z. *Tech. Phys.* **1931**, *12*, 593−604. (b) Tauc, J. *Mater. Res. Bull.* **1970**, *5*, 721−729.
(22) (a) Perdew, J.; Levy, P. M. *Phys. Rev. Lett.* **1983**, *51*, 1884−1887. (b) Yang, J.; Dolg, M. *J. Phys. Chem. B* **2006**, *110*, 19254−19263. (c) Lin, Z. S.; Kang, L. T.; Zheng, R.; Huang, H.; Chen, C. T. *Comput. Mater. Sci.* **2012**, *60*, 99−104.
(23) (a) Maggard, P. A.; Nault, T.; Stern, S. C. L.; Poeppelmeier, K. R. *J. Solid State Chem.* **2003**, *175*, 27−33. (b) Ok, K. M.; Halasyamani, P. S. *Inorg. Chem.* **2005**, *44*, 3919−3925. (c) Izumi, H. K.; Kirsch, J. E.; Stern, C. L.; Poeppelmeier, K. R. *Inorg. Chem.* **2005**, *44*, 884−895. (d) Kim, J. H.; Halasyamani, P. S. *J. Solid State Chem.* **2008**, *181*, 2108−2112. (e) Zhang, J. J.; Zhang, Z. H.; Zhang, W. G.; Zheng, G. X.; Sun, Y. X.; Zhang, C. Q.; Tao, X. T. *Chem. Mater.* **2011**, *23*, 3752−3761.
(24) (a) Brown, I. D.; Altermatt, D. *Acta Crystallogr.* **1985**, *B41*, 244−247. (b) Brese, N. E.; O'Keeffe, M. *Acta Crystallogr.* **1991**, *B47*, 192−197.